Proposal and Validation of a Knee Measurement System for Patients With Osteoarthritis

Riley Aaron Bloomfield, *Student Member, IEEE*, Megan Christine Fennema, Kenneth A. McIsaac, *Member, IEEE*, and Matthew G. Teeter

Abstract*—*Objective: **Currently most measurements of knee joint function are obtained through observation and patient-reported outcomes. This paper proposes an implementation and validation of a knee monitor to measure quantitative joint data in multiple degrees of freedom. The proposed system is configurable with minimal patient interaction and no frame-alignment calibration procedure is required for measurement after visually placing/replacing sensors on patients.** ***Methods:*** **A mobile software system was developed using a method of extracting clinical knee angles based on attitude estimations from independent wearable sensors. Validation was performed using a robot phantom and results were compared with a gold standard motion capture system. Two instrumentation placements (lateral and posterior) were examined.** ***Results:*** **A posterior sensor placement was determined to provide the most repeatable results through multiple degrees of freedom and measurement accuracy approached a gold standard motion capture technology with low root-mean-square error (flexion: 3.34°, internal/external rotation: 2.18°, and varus/valgus: 1.44°).** ***Conclusion:*** **The proposed system is simple to use and convenient for use in ambulatory or unsupervised environments for joint measurement; however, it was shown that accuracy can be sensitive to sensor placement.** ***Significance:*** **This system would be beneficial for obtaining quantitative patient data or tracking functional activity in variable environments, providing clinicians with indications of how patients' knees function during activity, potentially permitting more individualized care and recommendations.**

***Index Terms*—Knee measurement, wearable sensors, knee osteoarthritis, portable instrumentation.**

I. Introduction

OSTEOARTHRITIS (OA) is a common degenerative joint disease causing pain and discomfort during normal joint usage. It is the most common chronic condition of the joints, caused by deterioration of articular cartilage. Commonality of diagnosis is increasing alongside the average age of population and obesity rates. The disease is frequently diagnosed in the knee, hip, lower back, and neck, however knee OA is of particular concern; it has a higher rate of occurrence compared to other types of OA and it is prevalent in younger age groups [1], [2]. Symptoms include stiffness and discomfort whereas more severe cases introduce intense pain and limited function. Literature indicates that due to a lack of mobility, a large proportion of patients with knee OA do not meet physical activity guidelines which could increase the risk of diabetes, cancer and cardiovascular diseases [1], [3].

A. Total Knee Replacement

Total knee replacement (TKR) is reserved for more severe and progressed stages of knee OA. Medical advancements, implant material and design research, and improvements to surgical techniques have contributed to an overall increase in knee replacements performed annually. The number of recorded knee replacements in Canada alone has grown over 20% in the last five years with over 61,000 knee replacements performed in 2015. [4]. Joint replacement surgery is almost always successful in providing pain relief to patients and at least partially restoring joint function. Surprisingly, studies based on patient feedback reveal that a significant proportion of patients, up to one in five, are dissatisfied after TKR to the point of not undergoing the surgery again if it were an available option [5]–[7]. Multiple causes for this dissatisfaction have been suggested but a conclusion has not been reached. Surgical procedure, surgeon skill, implant selection, unrealistic patient expectations, joint function improvement, and individual joint qualities could all be contributing factors to patients' opinions of surgical success.

B. Functional Activity

Literature indicates improvement in functional activities such as stair-climbing, sitting cross-legged, and squatting strongly correlate with patient satisfaction [8], [9]. OARSI (Osteoarthritis Research Society International) has compiled a recommended list of performance-based tests used to assess physical function in patients diagnosed with knee OA [10]. Since performance of these tests can assess joint dysfunction, it would be expected that an improvement in performance would show joint treatment success. Traditional execution of these tests provides a start to end measurement (time taken, distance travelled) but fails

Manuscript received September 27, 2017; revised December 15, 2017 and March 13, 2018; accepted May 5, 2018. Date of publication May 16, 2018; date of current version January 18, 2019. This work was supported in part by The Arthritis Society, in part by the Ontario Early Researcher Award, and in part by the CIHR New Investigator Award. *(Corresponding author: Riley Aaron Bloomfield.)*

R. A. Bloomfield is with the Department of Electrical and Computer Engineering, Western University, London, ON N6A 5B9, Canada (e-mail: rbloomf@uwo.ca).

M. C. Fennema and M. G. Teeter are with the Department of Medical Biophysics, Western University.

K. A. McIsaac is with the Department of Electrical and Computer Engineering, Western University.

Digital Object Identifier 10.1109/TBME.2018.2837620

to identify information about joint usage intermediately. Aside from general activities, there are indications that certain knee performance capabilities could indicate the likelihood of satisfaction post-surgery. For example, flexion range has been shown to be an important indicator of surgical success whereas hyperextension has been associated with negative outcome measures [11]. An increase in knee flexion angle has also been presented to be an indicator of gait speed recovery, and demonstrates an increase in walking ability [12].

C. Patient Reported Outcome Measures

Patient reported outcome measures (PROMs) are widely used tools for obtaining qualitative feedback pre- and post-surgery. Measurements of health are obtained from patients' perspectives through surveys and questionnaires. A common example for hips and knees is the WOMAC patient questionnaire (Western Ontario and McMaster Universities Arthritis Index) [13]. This assessment method has been proven valid when administered over the phone, electronically, and through hard-copy in person, which greatly facilitates information retrieval [14]. While useful for registering patient data, this evaluation method fails to provide quantitative joint measurements. Additionally, if minor changes in health are unrecognized by the patient, they may not be reflected in reports.

Since TKR is almost always successful in reducing pain and restoring some function, PROMs often experience a ceiling effect which prevents discrimination between subtly different reports [15]. In addition, self-reported activity levels have been shown to differ from instrumented sessions, especially in overweight and obese patients [16]. Similarly, self-evaluated improvement in performance of activities does not correlate with objectively measured function in OA patients following joint replacement which emphasizes the need for quantitative instrumentation [17].

D. Current Measurement Tools

Current methods for measuring knee angles and usage such as instrumented gait analysis or camera-based measurements are expensive and must occur in testing environments that may not be easily accessible to patients. Since these traditional options require trained staff to operate, only limited data collection is feasible. Additionally, it has been indicated that a Hawthorne effect sometimes influences measurement accuracy when patients are being closely observed by an evaluator, which produces more ideal and less natural patient data than would normally be recorded if unsupervised [18], [19].

Continuous instrumentation of knee angles without constraining measurements to a specific environment would allow acquisition of quantitative joint metrics during usage without complex and obtrusive instrumentation. Information provided could accurately determine how individual patients use their joint by monitoring angles over time, potentially pre/post-surgery, and how this correlates to their satisfaction. This could identify key joint characteristics or functional activities that correlate to patient satisfaction using quantifiable metrics on a per-patient basis. With this knowledge, more individualized care can be provided to help promote satisfaction.

II. Background

A. Wearable Sensors

Wearable sensors are currently used in many industries including film animation, video game development, motion capture and medical instrumentation. Wearable systems can be small-sized and provide a viable method of instrumenting patients to assess surgical outcomes and detect movement disorders without constraining their environment [20]. A variety of wearable sensor types exist and can be split into two main categories: flexible materials and inertial units.

1) Flexible Materials: If tight fitting fabric can be worn by patients, flexible sensing materials provide an excellent option for obtaining joint angles. Multiple sensing fibres can be placed around body joints to accurately measure joint angles in multiple dimensions [21], [22]. These small fibres are lightweight but are limited by the physical length of the fibre; they cannot be separated. To measure joint angles, these devices must be mounted proximal to the affected joint and held in place, often with tight fitting materials or adhesives to prevent movement as the fibres stretch. This could cause discomfort for post-operative patients with joint swelling or pain. Similarly, digital goniometers have been used to determine joint angles with similar usage constraints [23], [24]. Goniometers produce low-noise and precise measurements but can be obtrusive for patients when combined to measure multiple degrees of freedom and their accuracy is dependent on correct sensor placement [20].

2) Inertial Units: An inertial measurement unit (IMU) is a micro-electromechanical system (MEMS) comprised of a gyroscope and an accelerometer. Most modern IMUs contain tri-axial components, allowing operation in three dimensions. Sensor fusion algorithms take raw gyroscope $(\mathrm{deg/s})$ and accelerometer $(\mathrm{m/s^2})$ readings and output an orientation estimation with respect to a calibrated coordinate system. Often the raw values of these devices can be queried independently to implement custom algorithms or set a defined local coordinate frame, such as the joint convention coupled to a body segment. Generally, IMUs produce drift over extended use if they do not return to rest allowing a true reading of gravity to be obtained.

Magnetic angular rate and gyroscope (MARG) sensors are similar to IMUs, but incorporate magnetometers. The additional reading is used to obtain the direction of Earth's magnetic field to help orient the sensor when external accelerations contribute to false accelerometer-based corrections. This hardware can generally obtain more accurate orientation estimates, but may be influenced by external magnetic interference [25], [26]. MARG sensors are also referred to as attitude and heading reference systems (AHRS) as they are used in aircraft and autonomous flight applications as a replacement for traditional mechanical attitude and heading devices [27].

Orientation estimations can be expressed in several ways; most commonly as rotational matrices, Euler angles, and quaternions. Rotational matrices contain redundant information and require more memory for computation so they are used less frequently in real-time or embedded systems. Euler angles provide a minimal representation of a change in rotation by using a three-step combination of rotations. Each independent stage is performed on a floating frame, so that following the first

rotation, the second is performed on the newly transformed frame, and the third rotation is performed on the frame resulting from the second rotation. Euler angle paramaterization is subject to a common singularity called Gimbal lock, occurring when one of the three combined rotations renders the frame in a parallel configuration where one axis becomes aligned with another, causing one degree of rotation to be coupled [26]. Quaternion representations are not inherently subject to singularities, allowing any rotation to be performed in a single step without reaching a parallel configuration. Many modern sensor fusion algorithms output estimations as unit quaternions [27]–[29].

B. Relevant Quaternion Theory

A quaternion is a minimal representation of a change in orientation originally described by William Hamilton [30]. This representation is commonly used in graphics and computer applications because of its avoidance to singular configurations and efficiency performing multiple rotations as linear combinations. It consists of only four numeric components, making it computationally and memory efficient.

A quaternion $\mathbf{q}$ representing a rotation $\mathbf{A}$ with respect to a global coordinate system $\mathbf{G}$ is defined as follows:

$$ {}^{G}_{A}\boldsymbol{q} = [q_0\ q_1\ q_2\ q_3]^T = a + b\hat{i} + c\hat{j} + d\hat{k} $$

where $\mathbf{a}, \mathbf{b}, \mathbf{c}, \mathbf{d}$ are real numeric components and $\hat{i}, \hat{j}, \hat{k}$ are orthogonal quaternion units.

A quaternion $\mathbf{q}$ can be related to a Cartesian coordinate frame through an extension of Euler's formula as:

$$ \mathbf{q} = \mathbf{e}^{\frac{\theta}{2}\left(u_x\hat{i}+u_y\hat{j}+u_z\hat{k}\right)} = \cos\frac{\theta}{2} + \left(u_x\hat{i} + u_y\hat{j} + u_z\hat{k}\right)\sin\frac{\theta}{2} \tag{1} $$

where θ is the magnitude of a rotation about the unit vector $\vec{u}$.

A non-zero unit quaternion $\mathbf{r}$ representing an orientation in 3-space can be obtained by normalizing a non-zero quaternion with the following equation:

$$ \mathbf{r} = \frac{r}{\|r\|} = \frac{q_0\ q_1\ q_2\ q_3}{\sqrt{q_0^2 + q_1^2 + q_2^2 + q_3^2}} \tag{2} $$

The conjugate of a unit quaternion $\mathbf{q}$ describing a rotation $\mathbf{A}$ with respect to $\mathbf{G}$ is equivalent to its inverse and is defined as:

$$ {}^{G}_{A}\boldsymbol{q}^* = {}^{A}_{G}\boldsymbol{q} = [q_0\ -q_1\ -q_2\ -q_3]^T \tag{3} $$

We define quaternion multiplication as a non-commutative combination of two rotations $\mathbf{q}$ and $\mathbf{r}$ as:

$$ q \otimes r = \begin{bmatrix} r_0q_0 - r_1q_1 - r_2q_2 - r_3q_3 \\ r_0q_1 + r_1q_0 - r_2q_3 + r_3q_2 \\ r_0q_2 + r_1q_3 + r_2q_0 - r_3q_1 \\ r_0q_3 - r_1q_2 + r_2q_1 + r_3q_0 \end{bmatrix} \tag{4} $$

III. Related Work

Activity monitors have become easily and readily available to the general public in many varieties. These devices include pedometers, accelerometers or full wearable systems designed to provide user feedback on exercise and activity levels. Many commercial products exist in the health care domain but to the authors' knowledge, there is no portable, practical, and economically feasible system for unconstrained instrumentation of the knee, measuring individual joint angles during usage in patients with OA.

A previously compiled report compared many common activity monitors used to monitor patients suffering with hip or knee OA [31]. The devices are shown to vary greatly in cost, hardware configuration, sample rate, interfaces, and data format. It was speculated that a sample rate as low as 25 Hz can be used to capture the movement of lower extremities [31]. Most interestingly, the devices are mounted to patients in many different ways: from ankle fixtures to wrist mounted sensors. Of the 14 devices specified in the report, none benefit from mounting a sensor above and below a patient's knee; the primary joint of interest. Systems are most commonly accelerometer based, using known acceleration pattern matching. Without estimating the orientation of each shank independently, certain metrics such as the amount of flexion in the knee while a patient is in an unexpected orientation such as laying on their back, for example, are not seen. Such movements may be common during physical therapy exercises and instrumentation of these sessions may be beneficial. Implementations with a single sensor do not provide sufficient information to identify knee asymmetries or changes in joint angles crucial to identifying knee-specific metrics.

In addition, IMU gait analysis solutions have been marketed to instrument functional testing of patients in a clinical setting [32]. These products fail to accurately measure knee flexion for unconstrained movements in patients with knee OA, which has been identified as a major usage characteristic contributing to patient satisfaction. It can be expected that accelerometer-only based systems using pattern matching techniques without recording independent orientations will fail to capture constant joint motion during slow activities or range of motion (ROM) exercises.

Systems specifically deriving joint angles from inertial units by combining accelerometer and gyroscope data currently exist [28], [29], [33]–[38]. The existing standard approach is to calibrate raw accelerometer and gyroscope data by performing procedures that require the patient to perform movements constricted to a single degree of freedom. During the constrained movements, the sensor frames are aligned to the attached body segment. It has also been shown that a known kinematic model of the joint can be used to measure angles between segments at high speeds by solving a non-linear observer problem. [38]. This method only requires that the sensors be at rest for alignment using a gravity vector. *El-Gohary et al.* show that this method is accurate (given several user specified parameters) through robotic testing. By contrast, the current work introduces a system which is not dependent on the attitude estimation algorithms used but relies only on quaternion sensor outputs without needing a kinematic model, reducing system computation drastically. Additionally, the world-coordinate readings readily provide information of a segment's position in the world to identify laying, standing or body turn directions during functional activity without more complex computation of body kinematics in future implementations. It should be noted that many existing systems are only tested on healthy subjects, mostly because they are early in development, and results could vary when testing

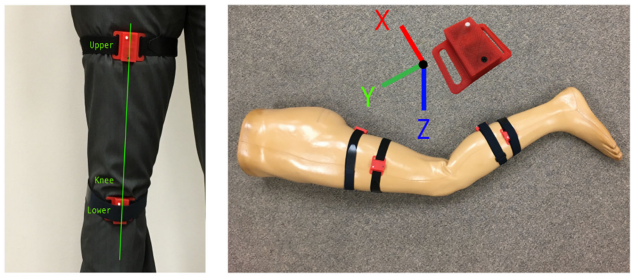

(a) (b)

Fig. 1. Sensors attached to a patient and a phantom leg. (a) Sensor attachment instruction for patients and clinicians. (b) Instrumented phantom leg (Sawbones Fully Encased Leg, Pacific Research Laboratories, Vashon, WA) with posterior and lateral placements and local sensor frame.

on unhealthy subjects [20]. Patients recovering from surgery may find these calibration procedures difficult. Many systems require the calibrations to be performed before every data collection session, every time the sensors are removed and replaced, or as frequently as possible [29], [33]–[35].

The proposed method of using independent attitude estimations from MARG sensors with respect to a global coordinate systems allows the sensors to be placed without any additional calibration. Since each sensor is responsible for its own attitude estimation, computing the difference in orientation is efficient and can be implemented using low-cost hardware.

IV. Methods

A. Implementation

As an input, the proposed system requires sensors capable of transferring or streaming quaternion attitude estimations wirelessly. MARG development boards (MetaMotionR, MBientLab, San Francisco, CA, USA) capable of estimating orientations using a self-contained sensor fusion algorithm at a rate of 25 Hz were obtained. Orientations are measured relative to a global left-handed frame defined identically for all manufactured sensors with the positive z-axis downward, the positive x-axis towards magnetic north and the negative-y axis orthogonal to the two former axes, calibrated in San Francisco, CA, USA. The boards and a rechargeable lithium-polymer battery were placed inside a custom PLA 3D-printed case (visible in Fig. 1(b)) approximately 1.2 cm thick, 3.0 cm wide, and 4.0 cm long. The case features two 1.5 cm wings extending from the sides for straps, and a concave back for patient comfort. Data are transferred over Bluetooth Low Energy (BLE) protocol to an Apple iPod Touch (fifth generation). An 8 MB on-board sensor memory chip was configured to store data objects without a persistent connection to a wireless device. The system proposed was implemented using the Swift 3.0 language developed for Apple devices.

B. Initialization

The system directs patients to attach the sensors using stretchable fabric hook and latch straps to their limbs as indicated in Fig. 1(a). The system then connects to four sensors (two on each limb of a patient) and once connected, indicates that they press the momentary push-button on each sensor in a specific order to localize the sensors to a body segment. Once pressed, the system will internally identify the sensor location for output and angle calculations. This interaction differs from a sensor calibration procedure because no constrained patient joint movement is required.

C. Motion Extraction Algorithm

Once the sensors are connected to the system wirelessly and their locations have been labelled internally, joint motion begins recording. The joint angles of each leg are calculated identically, but independently.

If we consider the quaternion orientation estimation read by the lower sensor with respect to its global coordinate system, it can be defined as:

$$ {}^{G}_{L}\boldsymbol{q} = [q_{l0}\ q_{l1}\ q_{l2}\ q_{l3}]^{T} $$

and similarly we can define the orientation of the upper sensor with respect to the same global coordinate system as:

$$ {}^{G}_{U}\boldsymbol{q} = [q_{u0}\ q_{u1}\ q_{u2}\ q_{u3}]^{T} $$

Note that either sensor frame could be used as a reference. The difference in orientation of the upper sensor with respect to the local coordinate frame of the lower sensor (chosen as a reference) can be found as:

$$ {}^{L}_{U}\boldsymbol{q} = {}^{G}_{L}\boldsymbol{q}^{*} \otimes {}^{G}_{U}\boldsymbol{q} \tag{5} $$

using the lower conjugate as defined in (3) and the linear combination defined in (4).

The difference in orientation ${}^{L}_{U}\boldsymbol{q}$ is now the single combined rotation from one segment's local frame to the other, with respect to the reference. To maximize this experiment's clinical relevancy and present results comparably to knee literature, ${}^{L}_{U}\boldsymbol{q}$ was transformed into flexion/extension (rotation in sagittal plane), internal/external (rotation in vertical plane), and varus/valgus (rotation in coronal plane) clinical angles using a Z-Y-X Euler sequence for lateral sensor measurements and a Y-Z-X Euler sequence for posterior sensor measurements. These sequences were motivated by performing the flexion rotation first because the majority of motion occurs about this sensor axis, varus/valgus second because the knee physically cannot reach $\pm 90\,\mathrm{deg}$ varus/valgus (rendering the rotation singular), and then the third remaining internal/external rotation about this transformed frame as has been done previously in literature [39]. Different sequences are required for each sensor placement despite calculating ${}^{L}_{U}\boldsymbol{q}$ identically since each sensor has a fixed local frame (visible in Fig. 1(b)) and when sensors are mounted differently about the knee, motions are reflected about different sensor axes.

D. Data Collection

As joint motion is computed using the algorithm above, data are simultaneously logged to the connected portable device and synchronized. The system recognizes a disconnect or communication failure with any of the attached sensors. In order to prevent data loss in this event, quaternions are simultaneously stored to

the on-board sensor memory to be retrieved by the application upon re-connection if a data synchronization error occurs from a lost connection. All data stored on-board or transferred to the portable device wirelessly are timestamped to allow merging of these two data storage methods to create a single synchronized data set.

E. Validation Experiment

To validate readings obtained by the proposed system, a robot phantom study was performed. A robotic manipulator was fitted with a mannequin leg (Fig. 1(b)) and was programmed to flex the leg starting completely extended (0 deg) through a linear path to approximately 120 deg for ten cycles with near-constant velocity. The upper limb was secured to a stationary apparatus and the manipulator end-effector was attached to the ankle. The manipulator and limb were placed inside a marker-based 3D motion gait lab (Cortex 2, Motion Analysis Corporation, Santa Rosa, USA) and fitted with reflective markers to provide a ground truth measurement for angles recorded during testing. Three independent tests were performed at two different speeds; slow (≈15 deg/s) and fast (≈25 deg/s). These testing speeds were limited by the maximum manipulator velocity at the end-effector. Two sensor pairs were attached in lateral and posterior positions on phantom limb as indicated in Fig. 1(b). The two simultaneous placements simulate two convenient placement options for sensors in patients with knee OA. Testing an anterior placement was not possible due to the anterior upper limb being blocked by the fixture apparatus. Between each of the three tests, all MARG sensors were completely removed from the phantom, shuffled randomly, re-positioned on the leg, and re-localized using the application specific push-button procedure. The placement and re-placement of the MARG units between tests simulates the removal and reattachment of sensors from patients. No calibration of the system was performed between tests or trials.

1) Data Collection: Data were collected using the custom developed mobile application. For this experiment, the synchronized data files were downloaded from the iPod and post-processed using Matlab (MathWorks, Natick, MA, USA) to ensure the integrity of data procured with an industry trusted software application. The analysis procedure from the proposed system was implemented using a Matlab script in addition to the original mobile Swift 3.0 implementation.

2) Data Analysis: Clinical angles were extracted from the sensor data using the proposed algorithm. Angles for the gold standard were found as an X-Z-Y Euler sequence that labels rotations in the same order with flexion as the first stage, then varus/valgus, and internal/external rotation as the final stage. Initial offsets were subtracted from data sets to align all tests to a common start for test-to-test comparison. No further filtering was performed on the data.

A cross correlation was used to determine if the posterior or lateral sensor placements provided the most repeatable path across multiple tests with device replacement. Tests were interpolated using the Matlab $interp1$ function to normalize timestamped test data from the same axis to the longest test set. This is necessary because sensor data streaming rates varied slightly when transferring across the wireless connection and data could not be exactly compared sample-to-sample. Correlation matrices comparing all three tests were computed using the Matlab function $f() = corrcoef(A, B)$ and the correlation coefficient was taken as the matrix diagonal $d(f(A, B))$. A mean measure of correlation **c** for each sensor placement option and the gold standard, for each degree of freedom was found using:

$$c_{axis} = \frac{d(f(t_1, t_2)) + d(f(t_2, t_3)) + d(f(t_1, t_3))}{3} \tag{6}$$

where t_n is the nth test at the same trial speed.

Since test correlations only compare the retest reliability and similarity of each placement, an average amplitude for all cycles of each test was computed as $amp_{test} = mean(peaks)$ to compare ranges in each axis of both placements to the gold standard, where $peaks$ is a set of all cycle amplitudes from complete extension to the cycle peak. A mean average of all tests at a single trial speed for each axis degree of freedom is found as:

$$amp_{axis} = \frac{\sum_{test=1}^{3} amp_{test}}{3} \tag{7}$$

To provide additional comparison of sensor placements to the gold standard, a value of root mean square error (RMSE) of each sensor test compared to its respective motion capture test was computed using the following equation:

$$RMSE(x, y) = \sqrt{\frac{1}{N}\sum_{n=1}^{N}(x(n) - y(n))^2} \tag{8}$$

where x, y are sensor data and gold standard data sets respectively, and N is the number of samples recorded. Note that all sensor test data sets were interpolated to gold standard tests for direct comparison using the Matlab $interp1$ function as done previously when computing cross correlations.

Finally, a measure of drift d_{test} was found by computing the change in amplitude between each successive cycle in a single test. The following Matlab equation was used: $d_{test} = mean(diff(peaks))$, where $peaks$ is a set of all cycle amplitudes from start to the cycle peak. A single mean value of drift for each placement option and the gold standard was found for each axis of rotation as the mean of all three test values.

V. Results

A. Path Correlation

Path correlations for each placement option and the gold standard through all tests can be seen in Figs. 2–4. The mean values calculated with (6) are shown in Table I along with their standard deviations. It can be seen that most paths were highly correlated, with less strong results showing a large standard deviation indicating that a single test may be lowering the mean. Flexion angle path correlations were the highest (1.00 ± 0.00 rounded to two decimal places) through both placements and speeds. Rotation angles have shown the lowest correlation, however, it should be noted that the overall amplitude of these rotations is low compared to other axes (mean of all placements ≈ 3.5 deg) as seen in Table II, so any small differences have a higher impact on correlation. Similarly, flexion amplitudes are large (≈120.0 deg) so noise and errors have a less significant effect on these path correlations.

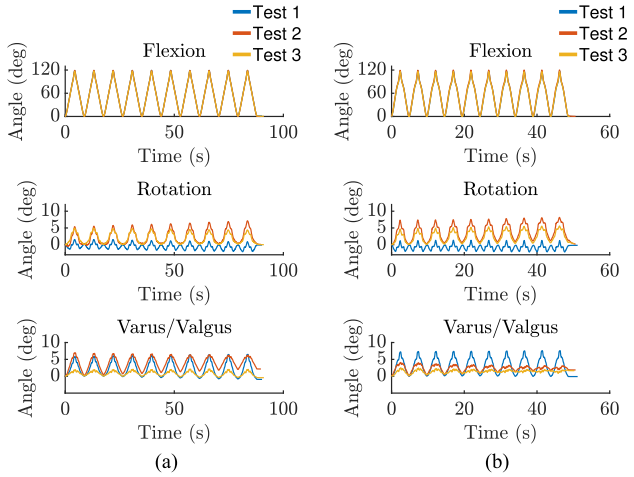

Fig. 2. Posterior sensor placement. (a) Slow speed. (b) Fast speed.

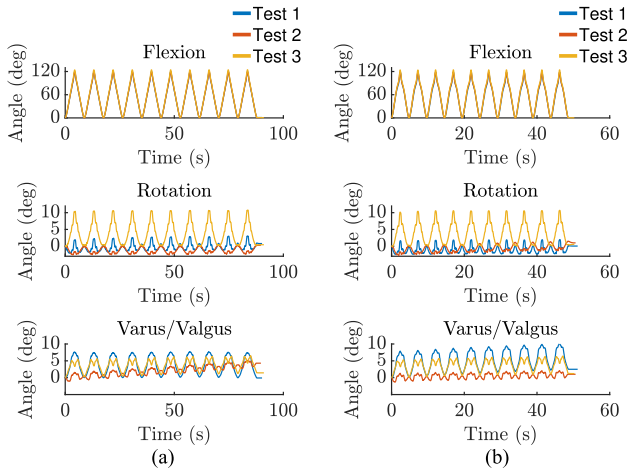

Fig. 3. Lateral sensor placement. (a) Slow speed. (b) Fast speed.

B. Path Amplitudes

Table II shows the mean sensor path amplitudes compared to the gold standard and their standard deviations computed with (7). Flexion angles were shown to be most accurate in comparison to the gold standard for both trial speeds with a mean difference in degrees of (lateral-slow: 1.39, posterior-slow: 1.23, lateral-fast: 0.40, posterior-fast: 2.24). Amplitudes of rotation and varus/valgus paths have shown large standard deviations (ranging from 2.51 deg to 5.48 deg) which indicates that sensor-body alignment could introduce non-negligible error in these axes during patient usage.

C. Root Mean Square Error

Table III shows the RMSE of each sensor test axis compared to the equivalent gold standard result calculated as shown in (8). The mean error of flexion tests was shown to be the largest (ranging from 3.29 deg to 3.52 deg), however, the range of motion in this axis was much larger. Varus/valgus showed low mean errors over three tests for both speeds (ranging from 1.42 deg to 2.30 deg). Mean errors of rotation varied more significantly

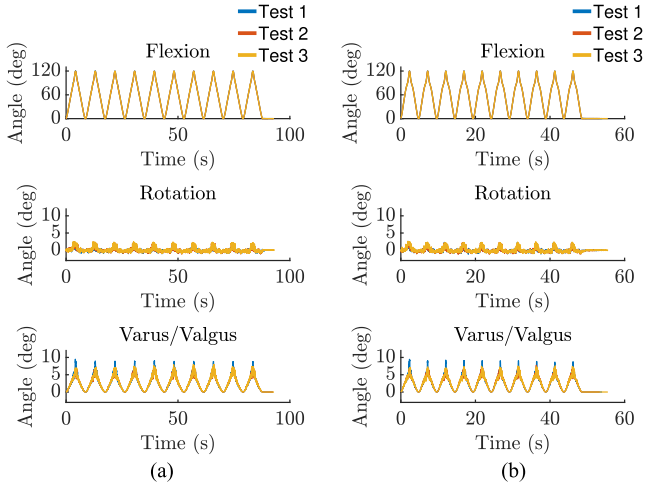

Fig. 4. Gold standard motion capture. (a) Slow speed. (b) Fast speed.

TABLE I
MULTI-TEST PATH CORRELATION

Slow	Lateral	Posterior	Gold Standard
Flexion	1.00 ± 0.00	1.00 ± 0.00	1.00 ± 0.00
Rotation	0.47 ± 0.34	0.68 ± 0.23	0.81 ± 0.08
Varus/Valgus	0.52 ± 0.31	0.92 ± 0.04	0.98 ± 0.01
Fast	**Lateral**	**Posterior**	**Gold Standard**
Flexion	1.00 ± 0.00	1.00 ± 0.00	1.00 ± 0.00
Rotation	0.45 ± 0.25	0.60 ± 0.35	0.83 ± 0.03
Varus/Valgus	0.67 ± 0.24	0.74 ± 0.14	0.98 ± 0.00

TABLE II
MULTI-TEST MEAN PATH AMPLITUDES

Slow	Lateral (deg)	Posterior (deg)	Gold Std. (deg)
Flexion	121.11 ± 2.92	118.49 ± 0.97	119.72 ± 0.33
Rotation	4.45 ± 5.48	4.04 ± 2.55	1.39 ± 0.76
Varus/Valgus	5.44 ± 2.63	4.92 ± 2.51	6.47 ± 0.43
Fast	**Lateral (deg)**	**Posterior (deg)**	**Gold Std. (deg)**
Flexion	120.39 ± 3.39	117.75 ± 1.92	119.99 ± 0.29
Rotation	4.41 ± 5.34	4.73 ± 3.23	2.14 ± 0.22
Varus/Valgus	5.63 ± 3.67	4.36 ± 2.75	7.70 ± 1.18

TABLE III
ROOT MEAN SQUARE ERROR TO GOLD STANDARD

Slow	Lateral (deg)			Posterior (deg)		
	Flex	Rot	Var	Flex	Rot	Var
Test 1	3.24	1.09	1.42	3.20	0.84	0.75
Test 2	3.66	1.80	2.08	3.68	2.71	1.49
Test 3	3.65	4.39	1.75	3.28	1.99	2.14
Mean	3.52	2.43	1.75	3.39	1.85	1.46
Fast	**Lateral (deg)**			**Posterior (deg)**		
	Flex	Rot	Var	Flex	Rot	Var
Test 1	4.43	1.37	2.75	4.02	0.97	0.78
Test 2	2.64	1.56	2.57	2.47	4.03	1.50
Test 3	3.41	4.24	1.58	3.38	2.49	1.98
Mean	3.50	2.39	2.30	3.29	2.50	1.42

between tests with a highest lateral error on test 3 (4.39 deg) and a highest posterior error on test 2 (4.03 deg) indicating rotation accuracy may be more influenced by placement when using the proposed rotation sequences.

D. Sensor Drift

The MARG sensors used in this study were in motion for $\approx$90 s at slow and $\approx$50 s at fast speeds without resting and in all tests there were only two occurrences of mean drift over 1 deg per ten-cycle test (slow-lat-var: 0.14 deg/cycle, fast-lat-var: 0.13 deg/cycle) It expected that OA patients will pause intermittently within this time frame (allowing a gravity vector to be found) so sensor accelerometer correction is expected to help accuracy. Magnetic disturbances were assumed to be minimal during this experiment but error could accumulate in real-world situations due to non-uniform magnetic interference.

VI. Discussion

Although the robot was programmed to flex through a linear path, non-negligible internal/external and varus/valgus rotation was observed in all tests. These additional motions are partly a result of the mannequin limb moving as a naturally constrained human leg, as well as soft tissue artifacts which are expected to be present during patient use (varying with leg size and muscle tone). Skin motion is a source of error in all external joint monitoring methods including gold standard gait systems and cannot be avoided using externally mounted sensors [40]. Despite some literature suggesting that additional motions can be ignored [33], [35], [41], knee motions such as varus/valgus thrust are important indicators in OA patients, indicating multi-dimensional measurement of the knee is significant [42].

Interpreting a quaternion as clinical angles is not trivial. Angle labels are assigned to rotations differently among literature, but they are often directly translated from three stages of independent local rotations constituting a traditional Euler representation. [35], [39], [43]–[45]. There are many three-stage, non-unique, and correct decompositions that can be found which makes the extraction of clinical angles dependent on the sequence. Interpretation is further dependent on the chosen reference segment. For example, when the knee is flexed, internal/external rotation occurring about the lower segment with an upper limb reference is a change in varus/valgus of the upper segment with a lower reference. For this study, the authors chose to use the upper limb as a reference for clinical angle extraction. Since motion capture measurements were made with respect to a stationary frame aligned with the upper limb, the upper segment was chosen as a reference for sensor computations because it moved less than 3 deg in all axes during testing for more equal comparison.

A consequence of computing the change in rotation with respect to a reference segment is that result accuracy will vary with alignment of the reference sensor to its body frame. An assumption of this system suggests that one of the sensors (reference) can be placed on a patient with correct alignment to the limb frame. Visual alignment has been previously tested with less than 5 deg error in a different wearable system [44]. Since the change of rotation is with respect to the reference frame, a misalignment of the non-reference sensor should not introduce error (kinematic crosstalk [46]) associated with knee motion occurring around a misaligned reference. Based on testing results, it is expected that poor alignment of the reference sensor will introduce this error. The authors suggest that correct placement is aided by the custom sensor case design used, which is elongated along the limb length, concave to conform and deter twisting, and held in-place using stretchable straps to prevent sensor liftoff. Further testing should take place concerning the correct attachment of a reference sensor to patients for improvement of rotation accuracy. Case design could be improved to accommodate wider straps to prevent the twisting of sensors against the skin. It can be seen in Fig. 1(b) that the straps used are more narrow than the 3D-printed slots on the red sensor cases. It is expected that at some placements, the sensors were able to rotate slightly independent of the straps during placement which should be avoided. Sensor fixation could be improved during patient usage by adding medical grade two-sided adhesive tape under the hook and latch straps.

In addition, further experimentation should consider an anterior sensor placement on patients for two reasons: the anterior lower limb could provide the better reference placement in patients since there is typically less soft tissue on the front of the shin, and this placement option would prevent patients from sitting on the sensors during activity.

Literature indicates that the standard error of measurement (SEM) in post-TKR patient flexion measured manually by experts is 4.1 deg while patient flexion has been shown to fluctuate up to 9.6 deg between measurements so system errors $\approx$4 deg can be declared clinically insignificant [47]. Wearable systems implemented using goniometers have been shown to produce $\approx 3-4$ deg of error during usage and previous inertial systems have reported RMSE of $\approx 2-4$ deg [20]. The experiment performed has shown that the three clinical angles can be extracted within these ranges of error.

Joint velocities of OA patients monitored may exceed the speeds tested in this study. The method of joint angle extraction was tested primarily, and similar accuracy at higher joint velocities will depend on the inertial sensors used, which have previously been shown capable of operating at more realistic velocities [20], [38].

VII. Conclusion

The proposed system using independent attitude estimations meets many of the desired qualities reported to be desirable in wearable systems for patients with OA, such as unobtrusiveness, small size, and low cost [48]. Minimal calibration facilitates usage for patients with limited mobility, making this tool appropriate for home, ambulatory, or clinical use as a replacement for more expensive instrumentation. All clinical angles have shown a low RMSE in degrees for both placements (flex: ≤ 3.52, rot: ≤ 2.50, var: ≤ 2.30) and low degree difference in mean cycle peaks (flex: 1.32, rot: 3.71, var: 2.00) compared to a gold standard, however, it has been mentioned that poor visual placement of the sensors could introduce larger error in practical use.

From these data, joint velocities and accelerations can be computed as well, potentially allowing for discovery of important knee parameters during patient usage. This proposed method

of computing joint angles using absolute attitude estimations can be used in any body orientation free of singularities, allowing knee joint monitoring through any scripted or unscripted activity.

REFERENCES

[1] B. Heidari, "Knee osteoarthritis prevalence, risk factors, pathogenesis and features: Part I," *Caspian J. Internal Med.*, vol. 2, no. 2, pp. 205–212, 2011.

[2] M. Cucchiarini *et al.*, "Basic science of osteoarthritis," *J. Exp. Orthopaedics*, vol. 3, no. 1, pp. 3–22, 2016.

[3] J. Wallis *et al.*, "What proportion of people with hip and knee osteoarthritis meet physical activity guidelines? A systematic review and meta-analysis," *Osteoarthritis Cartilage*, vol. 21, no. 11, pp. 1648–1659, 2013.

[4] Canadian Institute for Health Information, "Hip and knee replacements in Canada, 2014–2015: Canadian joint replacement registry annual report," Canadian Joint Replacement Registry, Can. Inst. Health Inf., Ottawa, ON, Canada, 2017. [Online]. Available: https://secure.cihi.ca/free_products/cjrr-annual-report-2016-en.pdf

[5] P. Noble *et al.*, "The John Insall award: Patient expectations affect satisfaction with total knee arthroplasty," *Clin. Orthopaedics Related Res.*, vol. 452, pp. 35–43, 2006.

[6] R. Bourne *et al.*, "Patient satisfaction after total knee arthroplasty: who is satisfied and who is not?" *Clin. Orthopaedics Related Res.*, vol. 468, no. 1, pp. 57–63, 2010.

[7] B. Chesworth *et al.*, "Willingness to go through surgery again validated the WOMAC clinically important difference from THR/TKR surgery," *J. Clin. Epidemiology*, vol. 61, no. 9, pp. 907–918, 2008.

[8] H. Du *et al.*, "Patient satisfaction after posterior-stabilized total knee arthroplasty: A functional specific analysis," *Knee*, vol. 21, no. 4, pp. 866–870, 2014.

[9] M. Furu *et al.*, "Quadriceps strength affects patient satisfaction after total knee arthroplasty," *J. Orthopaedic Sci.*, vol. 21, no. 1, pp. 38–43, 2016.

[10] F. Dobson *et al.*, "OARSI recommended performance-based tests to assess physical function in people diagnosed with hip or knee osteoarthritis," *Osteoarthritis Cartilage*, vol. 21, no. 8, pp. 1042–1052, 2013.

[11] M. Ritter, "The effect of postoperative range of motion on functional activities after posterior cruciate-retaining total knee arthroplasty," *J. Bone Joint Surg. Am*er., vol. 90, no. 4, pp. 777–784, 2008.

[12] Y. Y. Pua, "Factors associated with gait speed recovery after total knee arthroplasty: A longitudinal study," *Semin. Arthritis Rheumatism*, vol. 46, no. 5, pp. 544–551, 2016.

[13] N. Bellamy *et al.*, "Validation study of WOMAC: A health status instrument for measuring clinically important patient relevant outcomes to antirheumatic drug therapy in patients with osteoarthritis of the hip or knee," *J. Rheumatology*, vol. 15, no. 12, pp. 1833–1840, 1988.

[14] N. Bellamy *et al.*, "Osteoarthritis index delivered by mobile phone (m-WOMAC) is valid, reliable, and responsive," *J. Clin. Epidemiology*, vol. 64, no. 2, pp. 182–190, 2011.

[15] H. Behrend *et al.*, "The Forgotten joint as the ultimate goal in joint arthroplasty validation of a new patient-reported outcome measure," *J. Arthroplasty*, vol. 27, no. 3, pp. 430–436, 2012.

[16] M. Tully *et al.*, " Individual characteristics associated with mismatches between self-reported and accelerometer-measured physical activity," *PLoS One*, vol. 9, no. 6, 2014, Art. no. e99636.

[17] I. Luna *et al.*, "Early patient-reported outcomes versus objective function after total hip and knee arthroplasty," *Bone Joint J.*, vol. 99, no. 9, pp. 1167–75, 2017.

[18] A. Berman *et al.*, "Quantitative gait analysis after unilateral or bilateral total knee replacement," *J. Bone Joint Surg. Amer.*, vol. 69, no. 9, pp. 1340–1345, 1987.

[19] C. Malchow and G. Fiedler, "Effect of observation on lower limb prosthesis gait biomechanics: Preliminary results," *Prosthetics Orthotics Int.*, vol. 40, no. 6, pp. 739–743, 2016.

[20] P. Shull *et al.*, "Quantified self and human movement: A review on the clinical impact of wearable sensing and feedback for gait analysis and intervention," *Gait Posture*, vol. 40, no. 1, pp. 11–19, 2014.

[21] S. Yao and Y. Zhu, "Wearable multifunctional sensors using printed stretchable conductors made of silver nanowires," *Nanoscale*, vol. 6, no. 4, pp. 2345–2352, 2013.

[22] T. Trung and N. Lee, "Flexible and stretchable physical sensor integrated platforms for wearable Human—Activity monitoringand personal healthcare," *Adv. Mater.*, vol. 28, no. 22, pp. 4338–4372, 2016.

[23] A. Muro-De-La-Herran and B. Garcia-Zapirain, "Gait analysis methods: An overview of wearable and non-wearable systems, highlighting clinical applications," *Sensors*, vol. 14, pp. 3362–3394, 2014.

[24] N. Carbonaro *et al.*, "Exploiting wearable goniometer technology for motion sensing gloves," *IEEE J. Biomed. Health Informat.*, vol. 18, no. 6, pp. 1788–1795, Nov. 2014.

[25] J. Wu *et al.*, "Fast complementary filter for attitude estimation using low-cost MARG sensors," *IEEE Sensors J.*, vol. 16, no. 18, pp. 6997–7007, Sep. 2016.

[26] R. Valenti *et al.*, "A linear Kalman filter for MARG orientation estimation using the algebraic quaternion algorithm," *IEEE Trans. Instrum. Meas.*, vol. 65, no. 2, pp. 467–481, Feb. 2016.

[27] L. Zhao and Q. Wang, "Design of an attitude and heading reference system based on distributed filtering for small UAV," *Math. Probl. Eng.*, vol. 2013, pp. 1–8, 2013.

[28] A. M. Sabatini, "Estimating three-dimensional orientation of human body parts by inertial/magnetic sensing," *Sensors*, vol. 11, no. 2, pp. 1489–1525, 2011.

[29] F. Alonge *et al.*, "The use of accelerometers and gyroscopes to estimate hip and knee angles on gait analysis," *Sensors*, vol. 14, no. 5, pp. 8430–8446, 2014.

[30] S. W. R. Hamilton, *Elements of Quaternions*. London, U.K.: Longmans, Green, & Company, 1866. [Online]. Available: https://books.google.ca/books?id=b2stAAAAYAAJ

[31] M. Sliepen, M. Brandes, and D. Rosenbaum, "Current physical activity monitors in hip and knee osteoarthritis—A review," *Arthritis Care Res.*, vol. 69, no. 10, pp. 1460–1466, 2016.

[32] B. Greene *et al.*, "Fall risk assessment through automatic combination of clinical fall risk factors and body-worn sensor data," *IEEE J. Biomed. Health Informat.*, vol. 21, no. 3, pp. 725–731, May 2017.

[33] G. Cooper *et al.*, "Inertial sensor-based knee flexion/extension angle estimation," *J. Biomech.*, vol. 42, no. 16, pp. 2678–2685, 2009.

[34] J. Favre *et al.*, "Functional calibration procedure for 3D knee joint angle description using inertial sensors," *J. Biomech.*, vol. 42, no. 14, pp. 2330–2335, 2009.

[35] T. Seel *et al.*, "IMU-based joint angle measurement for gait analysis," *Sensors*, vol. 14, no. 4, pp. 6891–6909, 2014.

[36] H. Dejnabadi *et al.*, "A new approach to accurate measurement of uniaxial joint angles based on a combination of accelerometers and gyroscopes," *IEEE Trans. Biomed. Eng.*, vol. 52, no. 8, pp. 1478–1484, Aug. 2005.

[37] H. Dejnabadi *et al.*, "Estimation and visualization of sagittal kinematics of lower limbs orientation using body-fixed sensors," *IEEE Trans. Biomed. Eng.*, vol. 53, no. 7, pp. 1385–1393, Jul. 2006.

[38] M. El-Gohary and J. McNames, "Human joint angle estimation with inertial sensors and validation with a robot arm," *IEEE Trans. Biomed. Eng.*, vol. 62, no. 7, pp. 1759–1767, Jul. 2015.

[39] M. Kadaba *et al.*, "Measurement of lower extremity kinematics during level walking," *J. Orthopaedic Res.*, vol. 8, no. 3, pp. 383–392, 1990.

[40] C. Reinschmidt *et al.*, "Effect of skin movement on the analysis of skeletal knee joint motion during running," *J. Biomech.*, vol. 30, no. 7, pp. 729–732, 1997.

[41] M. Esch *et al.*, "Knee varus–valgus motion during gait a measure of joint stability in patients with osteoarthritis?" *Osteoarthritis Cartilage*, vol. 16, no. 4, pp. 522–525, 2008.

[42] A. Chang *et al.*, "Thrust during ambulation and the progression of knee osteoarthritis," *Arthritis Rheumatism*, vol. 50, no. 12, pp. 3897–3903, 2004.

[43] E. Grood and W. Suntay, "A joint coordinate system for the clinical description of three-dimensional motions: Application to the knee," *J. Biomech. Eng.*, vol. 105, no. 2, pp. 136–144, 1983.

[44] J. Favre *et al.*, "A new ambulatory system for comparative evaluation of the three-dimensional knee kinematics, applied to anterior cruciate ligament injuries," *Knee Surg. Sports Traumatology Arthroscopy*, vol. 14, no. 7, pp. 592–604, 2006.

[45] A. Sabatini, "Quaternion-based extended Kalman filter for determining orientation by inertial and magnetic sensing," *IEEE Trans. Biomed. Eng.*, vol. 53, no. 7, pp. 1346–1356, Jul. 2006.

[46] S. Piazza and P. Cavanagh, "Measurement of the screw-home motion of the knee is sensitive to errors in axis alignment," *J. Biomech.*, vol. 33, no. 8, pp. 1029–1034, 2000.

[47] P. W. Stratford *et al.*, "Modelling knee range of motion post arthroplasty: Clinical applications," *Physiotherapy Can.*, vol. 62, no. 4, pp. 378–387, 2010.

[48] E. Papi *et al.*, "A knee monitoring device and the preferences of patients living with osteoarthritis: A qualitative study," *BMJ Open*, vol. 5, no. 9, 2015.